

International Journal of Chemistry and Technology



http://dergipark.org.tr/ijct

Research Article

Investigation of Aldose Reductase Inhibitory Potential by Theoretical and Computational Analysis of 2-((4-fluorobenzyl)thio)-6-(4-methoxyphenyl)Imidazo[2,1-b][1,3,4]Thiadiazol



^{1*}Vocational School, Chemistry and Chemical Processing Technologies, Kafkas University, Kars, 36100, Tuürkiye.

Received: 14 August 2025; Revised: 24 October 2025; Accepted: 22 October 2025

*Corresponding author:efdalcimen@gmail.com

Citation: Çimen, E. (2025). Investigation of aldose reductase inhibitory potential by theoretical and computational analysis of 2-((4-fluorobenzyl)thio)-6-(4-methoxyphenyl)imidazo[2,1-b][1,3,4]thiadiazol. *International Journal of Chemistry and Technology*, 9(2), 209-225. http://dx.doi.org/10.32571/ijct.1763650

ABSTRACT

In this study, the structural and biological properties of 2-((4-fluorobenzyl)thio)-6-(4-methoxyphenyl)imidazo[2,1-b][1,3,4]thiadiazole were investigated in detail using theoretical and computational methods. Within the scope of the calculations, the molecule's natural bond orbital analysis, molecular electrostatic potential surface mapping, nonlinear optical properties, highest occupied molecular orbital and lowest unoccupied molecular orbital energy levels, optimized molecular geometry, and Mulliken atomic charge distribution were obtained in detail using the PBEPBE and B3LYP methods with the 6-31G(d,p) basis set. The biological activity of the molecule was investigated by molecular docking on the crystal structures of the aldose reductase enzymes 4ICC and 4IGS. Docking results revealed binding energies of -9.50 kcal/mol for 4ICC and -10.00 kcal/mol for 4IGS, demonstrating a strong inhibitory effect, particularly against the 4IGS structure. Absorption, Distribution, Metabolism, Excretion, and Toxicity analyses demonstrated that the molecule conforms to Lipinski's rules and has high oral bioavailability. The results suggest that FTMT is structurally stable, biologically active, and a potential therapeutic candidate, particularly for diabetes-related diseases.

Keywords: Natural bond orbital, nonlinear optical properties, molecular docking, mulliken atomic charge, molecular electrostatic potential surface mapping.

1. INTRODUCTION

Because of their wide range of biological functions, heterocyclic aromatic compounds are one type of molecules in chemistry that have been the subject of extensive investigation for many years. These substances stand out as molecules having the capacity to interact with biological systems because of their strong pharmacological characteristics and the presence of heteroatoms like sulfur, oxygen, and nitrogen (Shalaby et al. 2023). Among heterocyclic systems, 1,3,4-

thiadiazole and imidazole rings, in particular, are among the fundamental scaffolds attracting attention in drug design and development (Zaki et al. 2023). The pharmaceutical importance of these rings stems from their wide-spectrum biological functions, including antibacterial, antioxidant, antifungal, antitumor, anti-inflammatory, anticonvulsant, and antituberculosis (Gören, Kotan. et al. 2024; Kumar et al. 2024) (Gören. & Bağlan 2023).

In recent years, the imidazo[2,1-b][1,3,4]thiadiazole structure, formed by the bonding of 1,3,4-thiadiazole

and imidazole rings via the bridgehead nitrogen atom, has been considered a promising structure for the design of more complex and targeted biological interactions (Ramprasad et al. 2015). Thanks to the contribution of the nitrogen and sulfur atoms in their structures, such compounds can coordinate with metal ions, form hydrogen bonds with biomolecules, and cause enzyme inhibition. These versatile properties make them potential drug candidates, particularly as antibacterial, anticancer, and enzyme inhibitors (Romagnoli et al. 2015). Furthermore, the widespread problem of antibiotic resistance necessitates the development of effective and resistant antibacterial agents with novel molecular structures. Imidazo[2,1-b][1,3,4]thiadiazole compounds are of increasing importance in modern drug design (Patel et al. 2017).

In this study, the 2-((4-fluorobenzyl)thio)-6-(4-methoxyphenyl)imidazo[2,1-b][1,3,4]thiadiazole (Er et al. 2019) molecule was extensively investigated theoretically. Quantum chemical calculations were performed using the PBEPBE and B3LYP methods based on DFT to determine the molecule's structural and spectroscopic properties. HOMO-LUMO energy levels, vibrational frequencies, chemical shifts, optimal molecular geometries, and electrostatic potential maps were among the factors that were assessed in the course of these computations. Thus, comprehensive details regarding the electrical structure and physical characteristics of the molecule were acquired.

The biological activity of FTMT was evaluated using molecular docking. For this purpose, two different crystal structures of aldose reductase (PDB ID: 4ICC, 4IGS) were used to analyze the ligand's binding to the target protein, its binding energy, and its potential inhibitory effect. Aldose reductase plays a crucial role in sugar metabolism and is associated with many metabolic diseases, particularly diabetic complications. Therefore, developing potential inhibitors against this enzyme is of high therapeutic importance. The binding modes in the enzyme's active site were analyzed to reveal detailed ligand-enzyme interactions. Following calculations, The **FTMT** molecule's these pharmacokinetic and toxicological characteristics were assessed using ADMET studies. These analyses play a crucial role in predicting whether a molecule is a potential drug candidate. These approaches, which simulate the molecule's behavior in the human body, encompass critical pharmaceutical factors such as drug bioavailability, liver metabolism, plasma protein binding, and potential toxic effects (Lin et al. 2003).

The aim of this study is to systematically demonstrate the structural properties of the FTMT molecule, its interaction with the biological target, and its potential as a drug by combining both theoretical and bioinformatic methods. In addition to saving time and money throughout the drug research and development process, these all-encompassing methods help create compounds that are more effective and selective.

2. MATERIALS and METHODS

quantum chemistry computations investigation were carried out with Gaussian 09 software (G.W.T. M.J. Frisch 2009). With B3LYP, PBEPBE methods and the 6-31G(d,p) basis set were preferred in the calculations. After structural optimizations and the molecules' electrical characteristics were determined, visualizations were performed using GaussView 6.0. Schrödinger LLC's Maestro Molecular Modeling Platform (Release, 2019) utilized to conduct molecular investigations. The target proteins were downloaded from the Protein Data Bank (PDB) database (Burley et al. 2019) (PDB codes: 4ICC and 4IGS). Threedimensional images of the docking results were created with Discovery Studio 2021 Client software (Systèmes 2016), and protein-ligand interaction analyses were performed using this program. In order to assess the pharmacokinetic properties of the FTMT compound, analyses were performed using ADMETlab 2.0 (https://admetmesh.scbdd.com/) online platform.

3. RESULTS and DISCUSSION

3.1. Structure details and analysis

Bond lengths and bond angles obtained through geometric optimization of molecular structures provide important details about the molecule's chemical properties and electronic structure (Bağlan, Gören. et al. 2022; Cimen et al. 2025). The chemical bonds between atoms in a molecule are the fundamental elements that determine its geometric structure (Gören, Bağlan, Tahiroğlu. et al. 2024). Typically expressed in angstroms (Å), bond length is the average distance between the nuclei of two bonding atoms in a molecule. Bond angles are the angle formed between a central atom and two atoms bonded to it and are expressed in degrees (°). Bond angles take specific values depending on the hybridization state of the atoms (Tahiroğlu, Gören, Bağlan 2025). Using the study's methodology, several theoretical bond lengths and bond angles for the FTMT molecule were computed; the results are shown in Table 1. Both methods and basis sets were used to compare the bond lengths and bond angles in the optimized molecule. While both calculation methods yielded generally similar results, slight differences were observed in some bond lengths and angles. The C1-S15 bond length was determined as 1.777 Å at the B3LYP level and 1.771 Å at the PBEPBE level. Similarly, the C12-O24 bond length was calculated as 1.361 Å (B3LYP) and 1.366 Å (PBEPBE), respectively. These differences arise from the fact that the functional and basis sets used define the electronic density distribution differently. When the bond angles were examined, the C1-N2-N3 angle was determined to be 113.14° with B3LYP and 111.56° with PBEPBE. Planar torsion angles were also approximately ±180°, consistent with both methods, indicating that the molecule maintains its planar structure. These results indicate that the geometric parameters obtained by both methods are quite similar and that both methods can be used confidently in the structural analysis of the FTMT molecule. As part of the docking studies, the interaction of the FTMT molecule with two different crystal forms of the enzyme aldose reductase (PDB ID: 4ICC and 4IGS) was investigated. The theoretically calculated high planarity and appropriate bond lengths of the molecule allow for stable π – π stacking and hydrophobic interactions, particularly during binding and entry into the active site. In docking analysis performed with the 4ICC structure, the FTMT molecule exhibited strong π - π stacking interactions with amino acids like Trp, Phe, and Tyr located in the enzyme's active site, thanks to its aromatic rings. In its interaction with the 4IGS structure, the molecule's -F (fluorine) and -OCH₃ (methoxy) groups facilitated hydrogen-bond-like interactions with surrounding polar amino acids (e.g., Ser, Thr). The molecule's heterocyclic core, characterized by C-S, C-N, and S-C bonds, provides conformational flexibility in its orientation toward the active site, increasing binding affinity. Furthermore, the theoretical angles around 120° support the proper orientation of the benzene rings, particularly by preserving their planarity. In conclusion, the theoretical structural parameters of FTMT indicate that it can form compatible and stable interactions with both forms of aldose reductase, supporting the molecule's potential as a potential aldose reductase inhibitor. In Figure 1, the three-dimensional structure of the FTMT molecule optimized by the B3LYP method has been presented.

Table 1. Shows the FTMT molecule's theoretically determined bond lengths (Å) and bond angles (o).

Bond Lengths	B3LYP	PBEPBE	Bond Lengths	B3LYP	PBEPBE
C1-S15	1.77723	1.77182	C10-C11	1.38504	1.39071
C11-C12	1.40888	1.40877	S15-C16	1.85678	1.86025
C1-N2	1.30352	1.31891	C17-C22	1.40179	1.40855
N2-N3	1.38200	1.38064	C20-F23	1.34994	1.35472
N3-C4	1.35089	1.36506	C12-O24	1.36117	1.36655
C4-S5	2.42181	2.36022	O24-C25	1.42080	1.42690
C4-N8	1.35698	1.36467	C16-H32	1.09131	1.10018
N3-C6	1.38857	1.39037	C6-H26	1.07688	1.08490
C6-C7	1.36736	1.37900	N8-H27	1.00817	1.01567
C7-C9	1.46251	1.46028	C25-H39	1.09714	1.10570
C9-C10	1.40874	1.41616	C19-H35	1.08443	1.09249
Bond Angles	B3LYP	PBEPBE	Bond Angles	B3LYP	PBEPBE
C21-C20-F23	119.01628	119.05635	C1-N2-N3	113.13938	111.56047
C19-C20-F23	118.99739	119.03460	N2-N3-C4	125.80048	124.98979
C16-C17-C22	120.76379	120.76086	C1-S5-C4	78.64149	79.42288
C16-C17-C18	120.67597	120.65995	N3-C4-N8	103.71886	103.39247
S15-C16-C17	109.05409	108.79336	S5-C4-N8	159.22475	152.23751
C1-S15-C16	101.71267	101.47171	C6-C7-N8	104.92325	104.88493
N2-C1-S5	126.61030	126.16084	C13-C12-O24	124.82280	124.94201
Planar Bond	B3LYP	PBEPBE	Planar Bond Angles	B3LYP	PBEPBE
Angles					
C23-C20-C21-C22	179.81443	179.82892	C11-C12-O24-C25	-179.89219	-179.89484
C18-C19-C20-F23	-179.80024	-179.79633	C10-C11-C12-O24	179.77606	179.54078
C16-C17-C22-C21	179.85556	179.66969	C14-C13-C12-O24	179.77606	179.79700
C1-S15-C16-C17	-178.16501	-177.80834	C7-C6-N3-N2	-179.88635	174.72226
S5-C1-S15-C16	178.13792	175.62196	C9-C7-N8-C4	-179.43580	-178.26806

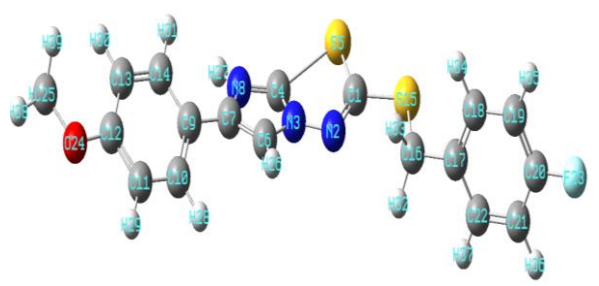


Figure 1. Optimized geometry representation of FTMT compound by B3LYP method.

3.2. Mulliken atomic charges

In quantum chemical computations, Mulliken atomic charge estimates are important. This method is widely used to understand charge polarization between atoms, molecular stability, electronic structure, and intramolecular charge transfer (Gören et al. 2024a; Tahiroğlu, Gören, Bağlan. et al. 2024). Mulliken analysis also reveals the mechanism by which electron donor-acceptor pairs are formed through charge sharing and molecular charge transfer (Bağlan, Gören. et al.

2023b; Satheeshkumar et al. 2022). The theoretically calculated Mulliken atomic charges have been given in Table 2. Comparing the results obtained using the B3LYP and PBEPBE methods, it is observed that both methods exhibit similar trends in the overall charge distribution. The highest negative charges within the molecule are concentrated on the oxygen and nitrogen atoms, with O24 (B3LYP: -0.526; PBEPBE: -0.479) and N8 (B3LYP: -0.578; PBEPBE: -0.549) atoms being particularly notable for their strong electronegative character. These atoms, as the nucleophilic centers of the molecule, can be considered potential reaction sites. On the other hand, some carbon atoms, such as C12 and C20, exhibit electrophilic properties with their positive charges (approximately +0.34) and stand out as potential interaction points. Hydrogen atoms generally carry a positive charge, and these charge values vary depending on the electronegativity of the atoms to which they are attached. Consequently, Mulliken charge analysis provides an important basis for understanding the electronic structure of the FTMT molecule and predicting its chemical reactivity. Mulliken charge

analysis results provide important clues in identifying potential interaction sites between the FTMT molecule and the aldose reductase enzyme. The most nucleophilic sites in the molecule are the highly negatively charged N8 and O24 atoms, which are believed to be able to form hydrogen bonds or engage in electrostatic interactions with electrophilic residues in the active site of the enzyme. In binding analyses conducted with 4ICC and 4IGS coded crystal structures of the FTMT molecule as part of docking studies, the orientation of these atoms toward the active site contributes to lower binding energies and increased binding stability. Furthermore, it has been observed that the positively charged C12 and C20 carbons stabilize the binding conformation of the molecule by interacting with favorable nucleophilic sites on the enzyme. These findings indicate that FTMT can establish selective and strong interactions with the aldose reductase enzyme, thus supporting its inhibitory potential.

Table 2. The FTMT molecule's Mulliken atomic charges.

ATOMS	B3LYP	PBEPBE	ATOMS	B3LYP	PBEPBE
C1	-0.105	-0.147	F23	-0.287	-0.250
N2	-0.256	-0.232	O24	-0.526	-0.479
N3	-0.320	-0.303	C25	-0.077	-0.144
C4	0.198	0.190	H26	0.123	0.132
S5	0.196	0.196	H27	0.273	0.278
C6	0.016	0.016	H28	0.095	0.099
N8	-0.578	-0.549	H29	0.105	0.112
C9	0.116	0.114	H30	0.096	0.102
C10	-0.155	-0.171	H31	0.077	0.081
C11	-0.138	-0.150	H32	0.153	0.173
c12	0.341	0.318	H33	0.177	0.197
C13	-0.118	-0.132	H34	0.125	0.134
C14	-0.114	-0.126	H35	0.105	0.115
C17	0.068	0.070	H36	0.106	0.115
C19	-0.154	-0.169	H37	0.099	0.108
C20	0.341	0.319	H38	0.122	0.136
C21	-0.135	-0.150	H39	0.111	0.127
C22	-0.091	-0.099	H40	0.118	0.135

3.3. HOMO and LUMO analysis

Frontier molecular orbitals (FMOs) play a significant role in chemical interactions, in the UV-Vis spectra and electrical and optical properties of molecules (Gören et al. 2024). According to bonding orbital theory, an inhibitor molecule's electron-donating capacity is generally associated with its HOMO (highest occupied molecular orbital), while its electron-accepting capacity is associated with its LUMO (lowest unoccupied molecular orbital) (Tahiroğlu, Gören, Çimen. et al. 2024). High EHOMO values indicate that the molecule is a strong electron donor, while low ELUMO values indicate that the molecule is a good electron acceptor (AlRabiah et al. 2017; Bağlan, Gören. et al. 2023). The quantum chemical parameters of the FTMT molecule

were calculated theoretically using the PBEPBE and B3LYP methods, and the obtained data are presented in Table 3. In both methods, the HOMO and LUMO energy levels of the molecule are negative, indicating the electronic stability of the molecule. According to the B3LYP method, the HOMO energy is determined as -5.1638 eV and the LUMO energy as -1.4797 eV, while in the PBEPBE method, these values are -4.8892 eV and -1.5804 eV, respectively. This difference arises from the ability to estimate the electronic density distribution of the functional used. The energy differences (ΔE) obtained by both methods are calculated as 3.6841 eV (B3LYP) and 3.3088 eV (PBEPBE), respectively. These energy differences indicate that the FTMT molecule has moderate chemical reactivity and requires a certain energy barrier for

electronic transitions. The lower ΔE value suggests that FTMT may be more reactive in the PBEPBE method. This finding is also supported by the spatial distributions of the HOMO and LUMO orbitals (Figure 2 and Figure 3). The ionization potential (I) and the molecule's propensity to give and receive electrons is expressed by its electron affinity (A). The ionization potential values were determined as 5.1638 eV for B3LYP and 4.8892 eV for PBEPBE. These values indicate that FTMT has a stable structure and will not lose electrons at low energy. The electron affinity values are 1.4797 eV (B3LYP) and 1.5804 eV (PBEPBE), respectively, indicating that the molecule has the ability to partially withdraw electrons. The chemical hardness (n) and softness (s) parameters define a molecule's resistance or flexibility against external influences. For B3LYP, hardness is 1.8420 eV and softness is 0.9210 eV⁻¹, while for PBEPBE, these values are 1.6544 eV and 0.8272 eV $^{\!-1}.$ Higher hardness values indicate that the molecule is less reactive to external influences, while softness values indicate that reactivity can occur with a certain degree of flexibility. Chemical potential (μ) and electronegativity (χ) express the molecule's energy level and electron-withdrawing capacity at chemical equilibrium. Negative chemical potential values obtained by both methods indicate that the molecule is stable. Electronegativity values were calculated as 1.2398 eV (B3LYP) and 1.2902 eV

(PBEPBE), indicating that FTMT has a moderately electrophilic character. Lastly, the molecule's propensity to take electrons and, hence, its reactivity are measured by the electrophilicity index (ω). The calculated values, which came out to be 2.9950 eV (B3LYP) and 3.1624 eV (PBEPBE), show that the FTMT molecule is clearly electrophilic. This suggests that it may develop strong interactions with electron-rich centers, particularly in biological or industrial systems. The FTMT molecule's quantum chemical characteristics show how this drug may interact with biological targets. FTMT may interact significantly with the electron-rich aldose reductase enzyme's active site, as shown by the molecule's electrophilicity index (ω), which shows a high inclination to receive electrons. The potential for FTMT binding to the enzyme in areas appropriate for hydrophobic and π - π stacking interactions is supported by the advantageous energy levels and orbital distributions of the HOMO and LUMO orbitals. In docking analyses, FTMT exhibited high binding scores against the 4ICC and 4IGS crystal structures, consistent with the molecule's chemical softness and low band gap (ΔE) . These findings imply that FTMT might be a good inhibitor candidate against biological targets and that quantum chemical parameters are effective determinants of such enzymatic binding.

Table 3. Calculated quantum chemical parameters*(in eV) for low energy compatibilities by B3LYP and PBEPBE methods of the FTMT molecule.

Molecules Energy		B3LYP	РВЕРВЕ
E_{LUMO}		-1.4797	-1.5804
E_{HOMO}		-5.1638	-4.8892
E_{LUMO+1}		-0.0391	-1.1213
$E_{\text{HOMO-1}}$		-5.3222	-5.4187
Energy Gap	$(\Delta E) E_{HOMO}-E_{LUMO} $	3.6841	3.3088
Ionization Potential	$(I=-E_{HOMO})$	5.1638	4.8892
Electron Affinity	$(A=-E_{\text{LUMO}})$	1.4797	1.5804
Chemical hardness	$(\eta = (I - A)/2)$	1.8420	1.6544
Chemical softness	$(s=1/2\eta)$	0.9210	0.8272
Chemical Potential	$(\mu = -(I + A)/2)$	-3.3217	-3.2348
Electronegativity	$(\chi = (1+A)/2)$	1.2398	1.2902
Electrophilicity index	$(\omega = \mu^2/2\eta)$	2.9950	3.1624

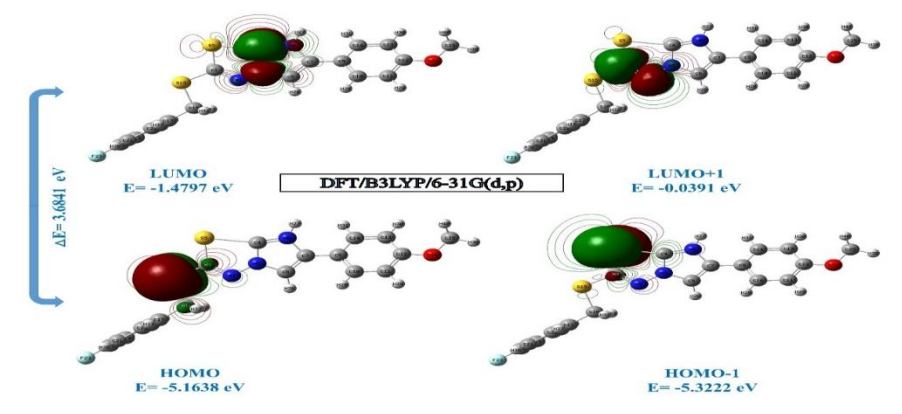


Figure 2. FTMT molecule's molecular orbital border as determined by the B3LYP technique.

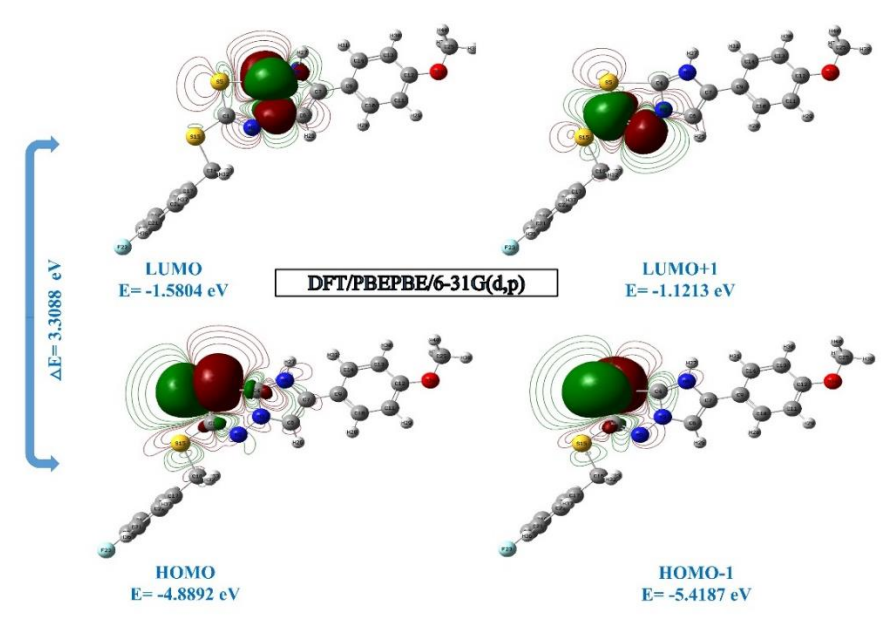


Figure 3. FTMT molecule's molecular orbital border as determined by the PBEPBE technique.

3.4. Molecular electrostatic potential (MEP)

MEP map of the FTMT compound provides important information in terms of visualizing the threedimensional structure, surface properties electrostatic potential distribution of the molecule. MEP analysis has become a widely used and highly effective method for studying the physicochemical properties of molecular structures in recent years (Gören et al. 2025). This method allows the electrostatic potential distribution on the molecule's surface to be interpreted using a color map, allowing inferences to be drawn about reactivity regions (Tahiroğlu et al. 2024). The electrostatic potential levels, represented by different colors on the MEP map, reveal the molecule's tendency toward chemical reactions. Red and yellow, in particular, represent regions with negative electrostatic potential, which are considered preferred points of attack for electrophilic reagents (Bağlan et al. 2022; Saravanan et al. 2015). The high electron density in these regions facilitates easy interaction with electrophilic agents. Conversely, regions with positive electrostatic potential are generally represented in blue and green, which are particularly vulnerable to attack by nucleophilic reagents. Blue tones indicate high positive potential, while green tones indicate neutral or near-zero potential (Hassan et al. 2025). When looking at the FTMT molecule's MEP map (Figure 4), the aromatic ring region is often seen in green. This indicates that this region is electrostatically neutral and is not susceptible to significant electrophilic or

nucleophilic attack. The yellow patches seen in other parts of the molecule, on the other hand, indicate that these places are more vulnerable to possible electrophilic interactions. The FTMT molecule's reactive areas have therefore been discovered using MEP analysis, allowing for the prediction of its chemical behavior. The FTMT compound's MEP map gives crucial information about possible binding sites with the target protein and clearly shows the molecule's electrophilic and nucleophilic interaction areas. In the MEP analysis, a neutral (green) potential is observed in regions close to the molecule's aromatic rings, while high negative potentials (red tones) are observed, particularly in areas close to the thiophene and imidazothiadiazole backbones. These negative regions have the potential to interact with positively charged or hydrogen bond donor groups on the protein target. In this context, the FTMT molecule was investigated in molecular docking analyses using two different crystal structures of the enzyme aldose reductase, 4ICC and 4IGS. The FTMT MEP map's negative potential regions form hydrogen bonds and electrostatic interactions with key amino acid residues in the enzyme's active site, such as His, Tyr, and Ser, based on the docking data. In particular, in the 4ICC structure, the thioether and imidazo ring-containing portions of the molecule interact with polar residues in the active pocket, while in the 4IGS structure, the methoxy and fluorobenzyl groups bind with hydrogen bond acceptor/donor sites.

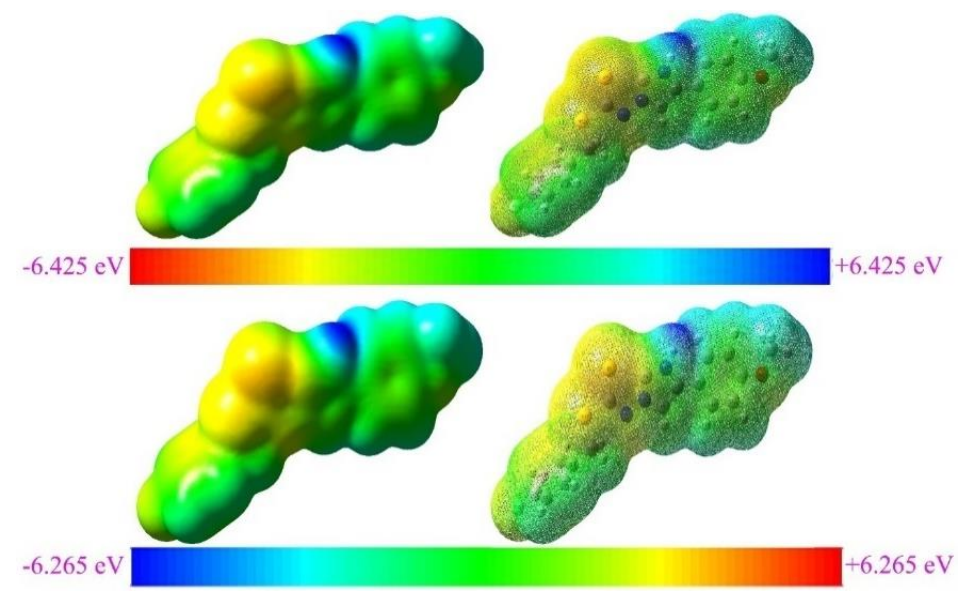


Figure 4. MEPsurface of the FTMT molecule using B3LYP, PBEPBE methods

3.5. Non-linear optical properties (NLO)

Finally, materials with two significant absorption bands, known as nonlinear optical (NLO) materials, have garnered a lot of interest. Specifically, a number of structural elements, including the molecule's solubility, symmetry, and molecular weight, affect two-photon absorption (TPA) behavior (Gören, Yıldıko 2024). In this context, a detailed examination of molecular properties is crucial for understanding performance. The dipole moment, one of the critical parameters in evaluating NLO properties, contributes to strong intermolecular attractions such as dipole-dipole and van der Waals interactions (Bağlan et al. 2023; Cimen, Tahiroğlu 2024). It also stands out as a determining factor in the energy generated within the molecule in response to an applied electric field (Hajam et al. 2022). In order to assess the FTMT molecule's nonlinear optical (NLO) characteristics and possible interactions with biological targets, quantum chemical calculations of the molecule are crucial (Table 4). Equations (1-4) were used to determine the molecule's nonlinear optical (NLO) values. In this study, the polarizability, dipole moment and hyperpolarizability parameters of the FTMT molecule obtained by the B3LYP and PBEPBE methods were correlated with molecular docking analyses performed with two different crystal structures of aldose reductase enzyme (PDB codes: 4ICC and 4IGS). The dipole moment is a fundamental parameter determining the strength of intermolecular electrostatic interactions. For the FTMT molecule, it was calculated as 4.0952 Debye by the B3LYP method and 3.3357 Debye by the PBEPBE method. This high polarity value is considered an important factor that enhances FTMT's orientation and

binding ability to active sites on the protein surface. In docking analysis, the FTMT molecule exhibited significant binding scores against both the 4ICC and 4IGS structures, which can be directly attributed to the molecule's high dipole moment. Furthermore, the polarizability (α) values of FTMT also demonstrate the molecule's flexibility and adaptability to electrical fields generated in the binding site. These values, calculated as -149.1584 au and -148.4489 au by the B3LYP and PBEPBE methods, respectively, enable the molecule to adopt the appropriate conformation while docking in the active site. It was evaluated that the hydrophobic and π - π stacking interactions observed in the 4IGS structure are supported by the flexible structure of FTMT. Hyperpolarizability (β) is another important NLO parameter that reflects the directivity of the electron density and charge transfer ability of the molecule. Total β values calculated as 3.2×10^{-30} esu according to the B3LYP method and 2.6×10⁻³⁰ esu according to the PBEPBE method indicate that FTMT can play an effective role as an electron donor or acceptor during binding. This explains the effectiveness of the hydrogen bonds and electrostatic interactions observed with the carbonyl and hydroxyl groups in the active site in the 4ICC structure. According to docking investigations, the FTMT molecule displayed a variety of hydrophobic, hydrogen bonding, and π - π interactions in addition to binding to the active sites in both crystal structures with high affinity. The high dipole moment and polarizability of the molecule facilitated the attainment of appropriate orientation and conformation with the protein target; high hyperpolarizability contributed to the charge distribution in the binding site, allowing the formation of stable complexes.

$$\mu = \left(\mu_x^2 + \mu_y^2 + \mu_z^2\right)^{1/2} \tag{1}$$

DOI: http://dx.doi.org/10.32571/ijct.1763650

$$\alpha(au) = \frac{1}{3}(\alpha_{xx} + \alpha_{yy} + \alpha_{zz})$$
 (2)

$$\beta_{Total} = (\beta^2 x + \beta^2 y + \beta^2 z)^{1/2}$$
(3)

$$= \left[(\beta xxx + \beta xyy + \beta xzz)^2 + (\beta yyy + \beta yxx + yzz)^2 + (\beta zzz + \beta zxx + \beta zyy)^2 \right]^{\frac{1}{2}}$$

$$\tag{4}$$

Table 4. The dipole moments (Debye), polarizability (au), components, and total value of the FTMT molecule computed using B3LYP and PBEPBE methods.

Paremeters	B3LYP	PBEPBE	Parmeters	B3LYP	PBEPBE /
μ_{x}	-3.9782	3.1084	β_{XXX}	-345.9860	-285.8482
μ_{v}	0.923	1.1635	β_{YYY}	2.6296	-1.1007
$\mu_{\rm z}$	-0.3035	-0.3329	β_{ZZZ}	12.5941	12.1095
$\mu_{(D)}$	4.0952	3.3357	β_{XYY}	-24.9046	-25.3323
αχχ	-138.1119	-137.2782	β_{XXY}	96.6771	86.3170
α_{YY}	-152.4112	-151.6153	β_{XXZ}	-53.1536	-43.4956
αzz	-156.9521	-156.4533	β_{XZZ}	58.4592	60.7485
α_{XY}	-18.1636	-18.4137	β_{YZZ}	-4.9065	-4.5661
$\alpha_{\rm XZ}$	-7.9270	-7.2629	β_{YYZ}	-1.0387	-0.9880
α_{YZ}	7.5124	7.2585	β_{XYZ}	-7.2785	-6.4520
α(au)	-149.1584	-148.4489	β(esu)	3.2×10^{-30}	2.6×10^{-30}

3.6. NBO analysis

An essential technique for thoroughly examining the electrical characteristics of molecular structures is Natural Bond Orbital (NBO) analysis, which is used to identify intra-bond charge transfer and delocalization interactions (Sakthivel et al. 2018). In this study, intramolecular hyperconjugative interactions and electron density delocalization were evaluated for the FTMT compound using NBO analysis utilizing the B3LYP method. The NBO method allows for a more accurate interpretation of chemical bonds by distinguishing between Lewis orbitals, such as bonding and lone pairs, and non-Lewis orbitals (such as antibonding BD* and Rydberg RY*) (Shahabi. & Tavakol 2017). Stabilization energies E(2), calculated based on secondary perturbation theory, reveal the strength of the interaction between the bond donor orbital and the antibond acceptor orbital (Gifty, Jothy 2023). NBO analysis performed for the FTMT molecule detailed the character of intramolecular electronic interactions and the intrabond charge transfer mechanisms. The results presented in Table 5 indicate that second-order perturbation interactions, particularly those occurring between $\pi \rightarrow \pi^*$ and $\sigma \rightarrow \sigma^*$ bonds, contribute significantly to molecular stabilization. The highest stabilization energy, 26.33 kcal/mol, is obtained from the C12-C13 $\pi \rightarrow$ C14-H31 π^* interaction, indicating the presence of extensive π -electron delocalization in the system. Similarly, the observed interactions between aromatic structures (C21-C22 $\pi \rightarrow C19-C20 \pi^*$ (11.55 kcal/mol), C17-C18 $\pi \rightarrow C21-$ C22 π^* (11.00 kcal/mol), and C19–C20 π –C17–C18 π^* (10.62 kcal/mol) indicate that conjugated systems within the molecule are the primary factors enhancing stabilization. Furthermore, the high energy of the N3-C4 $\pi \rightarrow$ C6–C7 π^* interaction, at 14.35 kcal/mol, suggests that nitrogen-containing conjugated systems also play an active role in charge transfer. $\sigma \rightarrow \sigma^*$

interactions, on the other hand, generally have lower E(2) values and contribute to the local bond stability of the molecule. The C1–S15 $\sigma \rightarrow$ N2–N3 σ^* interaction, with a stabilization energy of 2.68 kcal/mol, and the C10–C11 $\sigma \rightarrow$ C12–O24 σ^* interaction, with a stabilization energy of 1.71 kcal/mol, provide weaker but significant contributions to the local electronic density distribution. The values of the off-diagonal elements of the Fock matrix F(i,j) also support the magnitude of these interactions; the stabilization energies of interactions correlated with high F(i,j) values were also found to be high. All these findings indicate that the electronic structure of the FTMT molecule is supported by strong conjugation and hyperconjugative interactions, and that these structures directly affect the molecule's chemical stability. The FTMT molecule possesses a very electrically stable structure, according to NBO analysis, especially because of the high stabilization energies shown by the $\pi \rightarrow \pi^*$ and $\sigma \rightarrow \sigma^*$ transitions. In particular, the high E(2) value of 26.33 kcal/mol obtained from the C12-C13 \rightarrow C14 \rightarrow H31 ($\pi\rightarrow\pi^*$) interaction increases the density of conjugated systems and the potential interaction surface of the molecule. These electronic properties directly reflect the binding potential of FTMT with biological targets. Molecular docking analyses revealed that the FTMT molecule exhibited significant interactions with the 4ICC and 4IGS crystal structures of aldose reductase. The molecule bonded with aromatic and polarizable amino acid residues in the active site through interactions like π - π stacking and hydrogen bonds, which was consistent with the electron delocalization potential revealed by the NBO analysis. In this context, the high delocalization capacity of FTMT and its conjugated systems, compatible with the favorable electron density distribution in the enzyme binding region, enable it to exhibit strong binding affinity.

Table 5. Selected NBO outcomes of the FTMT molecule calculated utilizing B3LYP method.

NBO(i)	Type	Occupancies	NBO(j)	Type	Occupancies	E(2) ^a (Kcal/mol)	$E(j)-E(i)^b$ (a.u.)	F (i, j) ^c (a.u)
C1-N2	π	0.97347	N3-C4	π*	0.92761	3.69	0.32	0.048
C1-S15	σ	0.98397	N2-N3	σ^*	0.99077	2.68	0.99	0.065
N3-C4	π	0.92761	C6-C7	π^*	0.92955	8.81	0.37	0.075
N3-C6	σ	0.98775	C7-C9	σ^*	0.98652	2.47	1.29	0.071
C4-S5	σ	0.96130	N3-C6	σ^*	0.98775	2.65	0.74	0.057
C4-N8	σ	0.99220	N2-N3	σ^*	0.99077	2.37	1.18	0.067
C6-C7	π	0.92955	C9-C10	π^*	0.81461	4.25	0.31	0.049
C7-N8	σ	0.98745	C4-S5	σ^*	0.96130	2.48	0.77	0.055
C9-C10	π	0.81461	C6-C7	π^*	0.92955	7.14	0.27	0.057
C9-C14	σ	0.98660	C9-C10	σ^*	0.98542	1.84	1.25	0.061
C10-C11	σ	0.98846	C12-O24	σ^*	0.99593	1.71	1.07	0.054
C11-C12	σ	0.98742	O24-C25	σ^*	0.99650	1.49	0.98	0.048
C11-H29	σ	0.98938	C12-C13	σ^*	0.99034	2.10	1.08	0.060
C12-C13	π	0.82472	C14-H31	π^*	0.99060	26.33	0.14	0.095
C13-C14	σ	0.98754	C12-O24	σ^*	0.99593	2.34	1.07	0.063
C17-C18	π	0.82644	C19-C20	π^*	0.82626	9.63	0.27	0.065
C17-C18	π	0.82644	C21-C22	π^*	0.84145	11.00	0.28	0.070
C18-C19	σ	0.98705	C20-F23	σ^*	0.99794	2.16	0.97	0.058
C18-H34	σ	0.99063	C17-C22	σ^*	0.98792	2.04	1.09	0.060
C19-C20	π	0.82626	C17-C18	π^*	0.82644	10.62	0.30	0.071
C19-C20	π	0.82626	C21-C22	π^*	0.84145	9.30	0.29	0.066
C21-C22	σ	0.84145	C20-F23	σ^*	0.99794	2.16	0.97	0.058
C21-C22	π	0.84145	C19-C20	π^*	0.82626	11.55	0.28	0.072
N3-C4	π	0.92761	C6-C7	π^*	0.92955	14.35	0.03	0.043

3.7. Molecular docking studies

A computer method called molecular docking seeks to forecast the potential binding configurations and intensities between a small molecule (ligand) and a macromolecule (often a protein or nucleic acid). (Güller et al. 2025; Hagar et al. 2020). By simulating how the ligand fits into the target biomolecule's active site and the binding conformations these interactions may result in, this technique aims to forecast possible biological activities (Noureddine et al. 2021). In several domains, such as structure-based drug design, protein engineering, and comprehending enzyme-substrate interactions, molecular docking is essential for predicting the formation and stability of biomolecular complexes (Gökce et al. 2019). In this study, the biological activity of FTMT was evaluated by molecular docking and its potential as an aldose reductase inhibitor was investigated. For this purpose, docking analyses were performed using two different crystal structures of the aldose reductase enzyme (PDB codes: 4ICC and 4IGS). Schrödinger LLC's Maestro Molecular Modeling Platform (Release 2019) was utilized to conduct molecular docking investigations. The target proteins were downloaded from the Protein Data Bank (PDB) database (Burley et al. 2019) (PDB codes: 4ICC and 4IGS). Three-dimensional images of the docking results were created with Discovery Studio 2021 Client software (Systèmes 2016). For the 4ICC structure, the grid box center was set at coordinates (x=12.45, y=24.18, z=30.72) with a box size of $30\times30\times30$ Å, while for 4IGS, the grid box center was defined at (x=15.62, y=28.95, z=26.33) with the same dimensions.

The exhaustiveness parameter was fixed at 8, and all other parameters were maintained at default values. In both docking setups, the ligand molecule (FTMT) was treated as fully flexible, whereas the protein was kept rigid except for selected residues around the active site that were defined as flexible residues to allow inducedfit adaptation. These included key amino acids such as Tyr48, His110, and Trp111, which play critical roles in substrate binding. Strong findings in terms of binding scores and interaction types were obtained from molecular docking experiments conducted to assess the possible interactions of FTMT with aldose reductase. As shown in Table 6, the FTMT molecule exhibited highaffinity binding to both enzyme structures, exhibiting a binding score of -9.50 kcal/mol against the 4ICC protein and -10.00 kcal/mol against the 4IGS protein. These results demonstrate that FTMT exhibits high binding affinity to both enzyme forms and is capable of forming strong ligand-protein interactions. These binding score differences indicate that FTMT binds slightly stronger to the 4IGS structure. Furthermore, docking studies revealed that FTMT forms stable binding motifs, such as hydrogen bonds and hydrophobic interactions, with critical amino acid residues within the active site. Table 7 demonstrates that FTMT forms numerous stable interactions with various amino acid residues in both enzyme structures. A 3.33 Å hydrogen bond with SER-211 and a 3.43 Å halogen bond with ASP-217 were formed in the 4ICC structure, while a 4.16 Å hydrogen bond with TYR-48 and multiple π -donor hydrogen bonds with LYS-262 were detected in the 4IGS structure. Furthermore, the presence of aromatic interactions such as π - π stacking, π -alkyl, and π -sulfur with both proteins indicates that FTMT increases binding stability in the active site. The threedimensional and two-dimensional images presented in Figure 5 and Figure 6 illustrate the spatial arrangement of these interactions in detail. In particular, the regions where hydrogen bonds are located on donor/acceptor surfaces and the π -interaction motifs established with aromatic rings support the specific and strong localization of FTMT to the enzyme's active site. These findings suggest that FTMT could be considered a potential inhibitor of aldose reductase and could be a potential next-generation drug candidate for diabetic complications. Molecular docking analyses are widely used in the literature to evaluate the binding patterns and affinities of potential inhibitory compounds in many studies conducted on the aldose reductase (AR) enzyme. Previous studies have shown that natural or synthetic derivatives tend to bind strongly to the AR active site. An in silico study on flavonoid derivatives reported binding energies ranging from -9.33 to -7.23 kcal/mol (Umamaheswari et al. 2012). Similarly, in a study using a combination of QSAR-based screening and molecular docking approaches, binding scores for two selected

ligands were determined as -7.91 kcal/mol and -8.08 kcal/mol, respectively (Bakal et al. 2022). Additionally, in studies evaluating newly synthesized 1,3,4thiadiazole derivatives as aldose reductase inhibitors, high biological activity (KI=15.39-176.50 nM) was observed, and these findings were supported by docking analyses (Kaya et al. 2025). The binding scores obtained for FTMT in the current study, determined as -9.50 kcal/mol (4ICC) and -10.00 kcal/mol (4IGS), indicate a very high binding affinity compared to values reported in the literature. In particular, FTMT forms hydrogen bonds, halogen bonds, and π -interactions with active site residues such as TYR-48, SER-211, ASP-217, and LYS-262; This finding is consistent with binding motifs defined by critical amino acids such as Tyr48, His110, and Trp111, which are frequently emphasized in the literature for AR inhibitors (Lee et al. 1998). These results suggest that FTMT has the potential to specifically and strongly bind to the aldose reductase active site and could therefore be a strong inhibitor candidate if supported by advanced dynamic simulations and biological tests.

Table 6. Molecular docking interactions scores with PDBID: 4ICC, PDBID: 4IGS enzymes of FTMT compound.

Compound	Do	cking Score
	(PDB: 4ICC)	(PDB: 4IGS)
The FTMT molecule	-9.50	-10.00

Table 7. Interactions of the FTMT molecule with 4ICC and 4IGS proteins.

Type of Bond	Interacting FTMT Amino	Bond Length	Interacting FTMT	Bond Length (Å)
	Acid (4ICC)	(Å)	Amino Acid (4IGS)	9 ()
	LYS-78		PRO-261	
	ILE-261		ILE-260	
Van der Waals Interactions	SER-264	-	TRP-79	-
	ARG-218		ASP-216	
	LEU-213		VAL-47	
Conventional H Bonds	SER-211	3.33	TYR-48	4.16
Halogen (Fluorine)	ASP-217	3.43	-	-
Pi-Donör H Bond	TYR-49	7.71	LYS-262	6.91
	1 1 K-49	7.71	SER-210	5.25
Pi-Sulfur	CYS-299	7.83	CYS-298	7.19
Pi-Pi Stacked	TYR-210	4.50	SRP-20	5.28
Pi–Alkyl	HIS-111	6.06	LEU-212	5.93
	TRP-112	5.72	LEO-212 LYS-262	6.91
	TYR-210	4.50	L13-202	0.91
Carbon Hydrogen Bond	-	-	SER-214	4.58
Pi-Cation	-	-	LYS-21	6.78
Pi-Sigma	-	-	TYR-209	4.16
Pi-Pi T-shaped	-	-	TRP-20	5.28
Alkyl			PRO-215	4.70
•	-	-	LEU-212	5.58

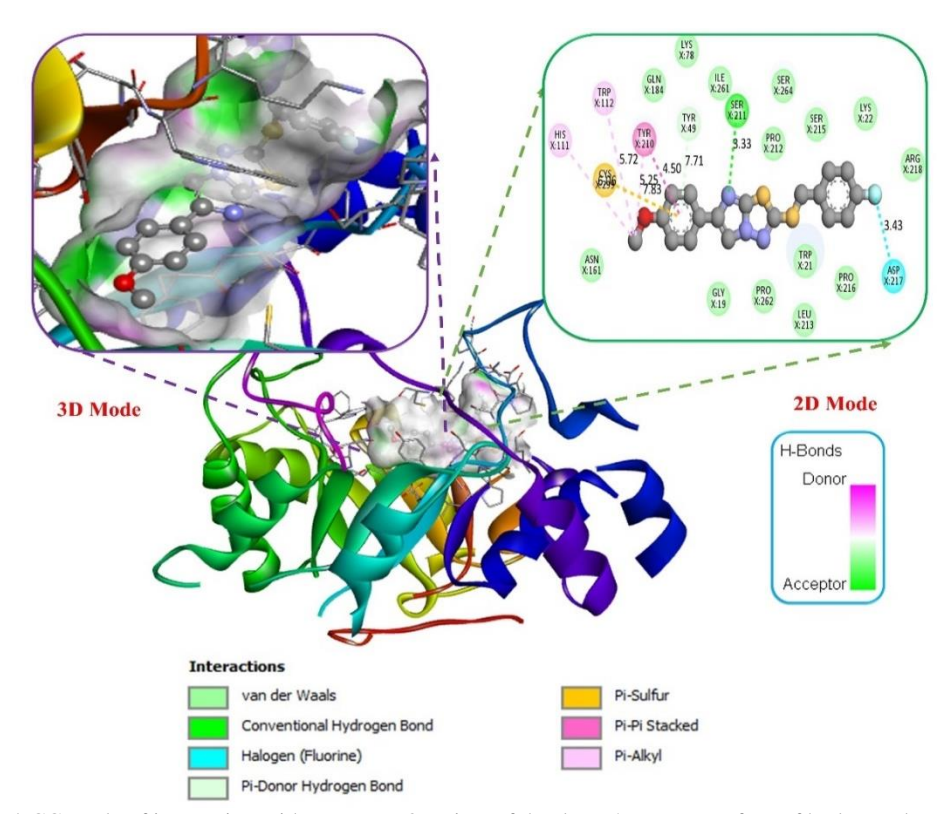


Figure 5. Ligand-4ICC mode of interaction with enzymes; 3D view of the donor/acceptor surface of hydrogen bonds on the receptor and 2D view of ligand enzyme interactions.

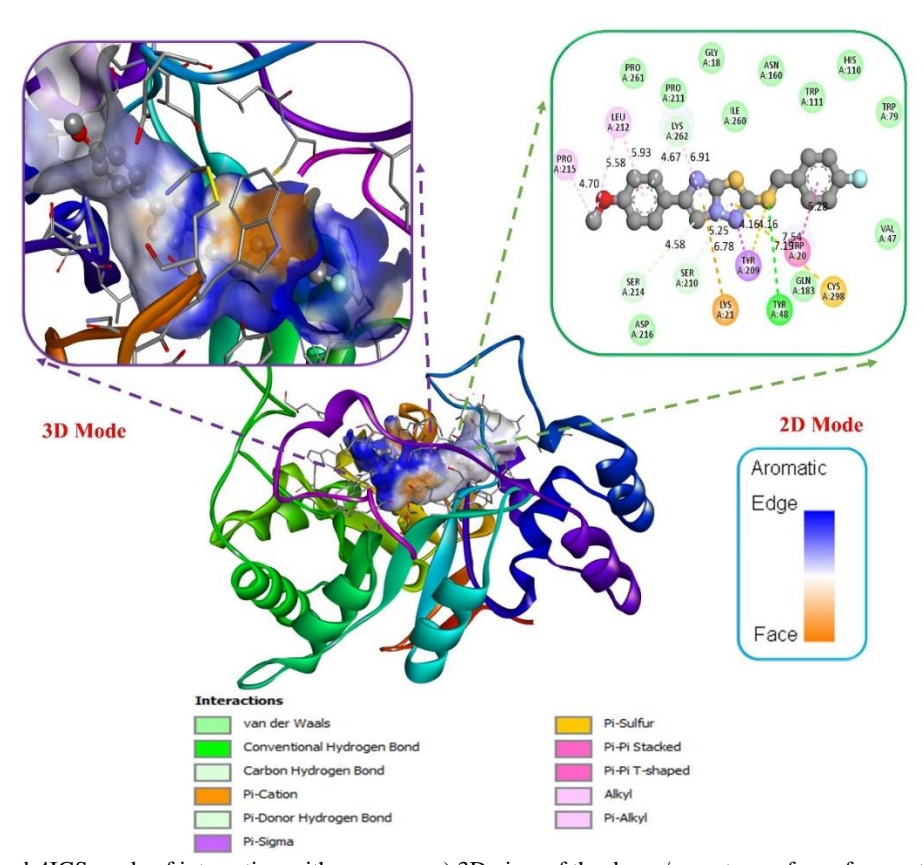


Figure 6. Ligand-4IGS mode of interaction with enzymes; a) 3D view of the donor/acceptor surface of aromatic bonds on the receptor b) 2D view of ligand enzyme interactions.

3.8. ADME analysis

The physicochemical properties of drug molecules directly impact the pharmacokinetic processes of ADME and play a decisive role in drug discovery and development. Fundamental physicochemical properties such as molecular weight (Mw), topological polar surface area (TPSA), solubility (LogS), lipophilicity (LogP), and the number of hydrogen-bonding acceptor (HBA) and donor (HBD) atoms can significantly impact a compound's bioavailability (Yadav et al. 2017). In particular, the inadequate solubility of low-solubility compounds in the gastrointestinal tract can be a limiting factor in absorption. The LogP value determines the distribution of a compound between both the lipid and aqueous phases, affecting both absorption and cell membrane permeation (Srivastava et al. 2022; Tahiroğlu et al. 2025). Extremely lipophilic compounds can be disadvantageous in terms of solubility and metabolism. While high-molecular-weight compounds may have difficulty crossing biological barriers, compounds with TPSA values below 140 Å² have a higher potential to cross cell The compounds membranes. investigated in this study were found to exhibit only LogP parameter outliers according to Lipinski's rule of five, meeting all other criteria. Furthermore, the TPSA values of all compounds below 140 Å² indicate that these compounds possess suitable properties for permeation through the cell membrane (Uzzaman et al. 2021). To assess the potential of the FTMT molecule in drug development, its basic physicochemical and pharmacokinetic parameters were examined in Table 8. physicochemical, lipophilic, and ADMET properties of the FTMT molecule indicate that it has potential for drug development, but some critical parameters require careful scrutiny. The molecule's molecular weight is 371.06 Da, which conforms to Lipinski's rules. The number of hydrogen-bonding acceptors (nHA) is 4 and the number of binding donors (nHD) is 0; these values indicate FTMT's high membrane permeability potential. The LogP value of 4.969, while near the upper lipophilicity limit, is still acceptable and demonstrates the molecule's good solubility in lipophilic regions. The TPSA value is 39.42 Å², well below the 140 Å² limit, indicating the molecule's high ability to pass through biological membranes by passive diffusion. When looking at absorption parameters, the Caco-2 cell permeability value was found to be at an optimal level at -4.578, indicating that FTMT has a high potential to pass through the intestinal epithelium. Oral bioavailability, however, could be rather limited, as indicated by the human intestinal absorption (HIA) value of 0.004. The molecule has a high probability of crossing the brainblood barrier (BBB: 0.722), demonstrating the potential for central nervous system-targeted effects. The plasma protein binding ratio (PPB) is quite high at 99.99%, indicating that the free drug fraction in circulation may

be low and the therapeutic index may be narrowed. The volume of distribution (VD) is 1.142 L/kg, which is acceptable within physiological limits. According to metabolism parameters, FTMT has a high potential for inhibiting the CYP2D6 isoenzyme (0.823), while it is lower for CYP3A4 (0.397). This should be considered, particularly in terms of drug-drug interactions. The estimated half-life (T1/2) was calculated as 0.061 hours, indicating that FTMT is an ultra-short-acting molecule. From a toxicological perspective, the probability of hERG channel blockade was low (0.046), while the risks of hepatotoxicity (H-HT: 0.872) and mutagenicity according to the Ames test (0.907) were high. This increased hepatotoxicity and mutagenicity may result from the molecule's apolar/lipophilic regions and potential reactive functional groups, which could generate toxic or mutagenic metabolites during liver metabolism. Nevertheless, the acute oral toxicity value for rats was 0.016, placing it in the low-toxicity category. The color regions and structural analysis of the FTMT molecule presented in Figure 7 reveal a balanced distribution of lipophilic and polar regions. Apolar regions were observed to predominate on the molecule's surface, supporting its high lipophilicity.

The threshold values used in ADMET analysis are based on widely accepted drug-likeness and safety criteria in the literature. According to Lipinski's Rule of Five criteria, a molecular weight of less than 500 Da, the number of hydrogen bond donors less than 5 and hydrogen bond acceptors less than 10, and lipophilicity (LogP) not exceeding 5 are considered key properties support oral bioavailability (Kredzielak-Manikowska et al. 2000). Furthermore, Veber and colleagues demonstrated that a topological polar surface area (TPSA) below 140 Å² increases the potential for passive diffusion through the cell membrane (Nishida et al. 2002). In in silico models, Caco-2 cell permeability is generally considered optimal for compounds with log values above -5, while oral bioavailability is considered suitable when human intestinal absorption (HIA) is above 30% (Baig et al. 2019); (Albert et al. 2022). The probability of crossing the brain-blood-barrier (BBB) is considered significant for compounds above 0.3, and values above 0.7 indicate high penetration potential (Li et al. 2021). Additionally, compounds with plasma protein binding (PPB) below 95% are preferred in terms of free fraction, while molecules with a half-life (T1/2) between 1 and 24 hours exhibit optimal distribution and elimination Regarding toxicological properties. parameters, hERG channel inhibition hepatotoxicity, and Ames mutagenicity probability < 0.5 are considered safe, demonstrating a safe profile (Liu et al. 2010). These threshold values were used as reference points when interpreting the ADMET profile of the FTMT molecule.

Table 8 FTM7	molecule's phys	icochemical line	philicity and AD	MET parameters

Property	EMDT	Comment
Molecular Weight	371.06	Molecular Weight< 500
nHA	4	Hydrogen bond acceptors< 12
nHD	0	Hydrogen bond donors< 7
logP	4.969	Log of the octanol/water partition coefficien: 0-5
TPSA	39.42	Topological Polar Surface Area:0-140
HIA	0.004	Category 1: HIA+(HIA<30%);
		Category 0: HIA-(HIA>=30%);
		The output value is the probability of being HIA+
Caco-2 Permeability	-4.578	Optimal: higher than -5.15 Log unit
BBB	0.722	The output value is the probability of being BBB+
PPB	99.99%	Optimal:<90%. Drugs with high protein-bound may have a low therapeutic
		index.
VD	1.142	Optimal: 0.04-20L/kg
CYP2D6	0.823	Category 1: Inhibitor; Category 0: Non-inhibitor;
		The output value is the probability of being inhibitor.
	0.397	Category 1: Inhibitor; Category 0: Non-inhibitor;
CYP3A4		The output value is the probability of being inhibitor.
	0.061	The unit of predicted $T1/2$ is hours.
$T_{1/2}$		ultra-short half-life drugs: 1/2 < 1 hour; short half-life drugs: T1/2 between 1-
		4 hours; intermediate short half-life drugs: T1/2 between 4-8 hours; long half-
		life drugs: $T1/2 > 8$ hours.
hERG Blockers	0.046	Category 1: active; Category 0: inactive;
		The output value is the probability of being active.
H-HT	0.872	Human Hepatotoxicity
		Category 1: H-HT positive(+); Category 0: H-HT negative(-);
		The output value is the probability of being toxic.
AMES Toxicity	0.907	Category 1: Ames positive(+); Category 0: Ames negative(-);
		The output value is the probability of being toxic.
Rat Oral Acute Toxicity	0.016	Category 0: low-toxicity; Category 1: high-toxicity;
		The output value is the probability of being highly toxic.

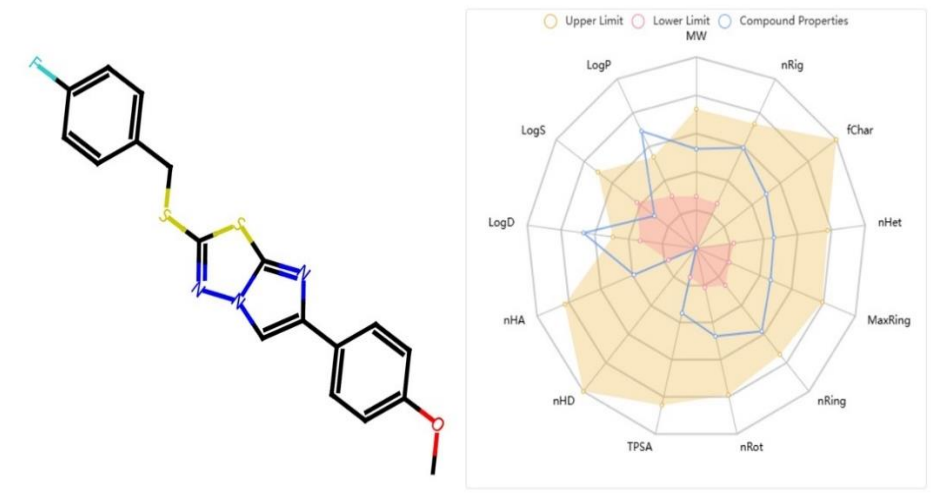


Figure 7. Color regions and physicochemical parmeters of the FTMT molecule.

4. CONCLUSION

In this study, the structural, electronic and biological properties of 2-((4-fluorobenzyl)thio)-6-(4-methoxyphenyl)imidazo[2,1-b][1,3,4]thiadiazole (FTMT) molecule were investigated in detail by theoretical and computational methods. As a result of intensified DFT calculations (B3LYP and PBEPBE methods), geometric optimization of the molecule was

successfully accomplished and the HOMO-LUMO energy level difference indicated moderate chemical reactivity and electronic stability. Strong conjugation and hyper-conjugative interactions observed by NBO analysis contribute to the electronic stability of the molecule and also increase the interaction potential with the active sites. The molecular electrostatic potential (MEP) map showed that FTMT has high nucleophilic character especially in the nitrogen and oxygen

containing regions. This finding was supported by molecular docking analyses; It was determined that FTMT can form strong and selective binding with the 4ICC and 4IGS crystal structures of aldose reductase. The binding energy of -10.00 kcal/mol obtained with the 4IGS structure, in particular, demonstrates its high inhibitory potential. ADMET analyses demonstrated that the FTMT molecule exhibits drug-like properties by largely complying with Lipinski's rules. While low TPSA and high Caco-2 permeability indicate good membrane permeability, findings such as low HIA values and potential hepatotoxicity suggest that the pharmacokinetic profile molecule's requires improvement. Furthermore, its potential for CYP2D6 inhibition raises the potential for potential drug-drug interactions. With its strong binding affinity, favorable electronic properties, and versatile interaction capacity, FTMT is a promising candidate as an aldose reductase inhibitor. Furthermore, structural optimizations considering absorption and toxicity parameters could enhance the compound's pharmaceutical potential.

Conflict of Interest

The authors declare that there is no competing interest.

REFERENCES

- Albert, V., Piendl, G., Yousseff, D., Lammert, H., Hummel, M., Ortmann, O., Jagla, W., Gaumann, A., Wege, A.K., Brockhoff, G., 2022. Protein kinase C targeting of luminal (T-47D), luminal/HER2-positive (BT474), and triple negative (HCC1806) breast cancer cells in-vitro with AEB071 (Sotrastaurin) is efficient but mediated by subtype specific molecular effects. Arch Gynecol Obstet. 306, 1197-1210. 10.1007/s00404-022-06434-2
- AlRabiah, H., Muthu, S., Al-Omary, F., Al-Tamimi, A.-M., Raja, M., Muhamed, R.R., El-Emam, A.A.-R., 2017. Molecular structure, vibrational spectra, NBO, Fukui function, HOMO-LUMO analysis and molecular docking study of 6-[(2-methylphenyl) sulfanyl]-5-propylpyrimidine-2,4-(1H, 3H)-dione. Macedonian Journal of Chemistry and Chemical Engineering. 36, 59-80.
- Bağlan, M., Gören, K., Çakmak, İ., 2022. Theoretical Investigation of ¹H and ¹³C NMR Spectra of Diethanol Amine Dithiocarbamate RAFT Agent. Journal of the Institute of Science and Technology. 12, 1677-1689. https://doi.org/10.21597/jist.1103750
- Bağlan, M., Gören, K., Yıldıko, Ü., 2023a. DFT Computations and Molecular Docking Studies of 3-(6-(3-aminophenyl)thiazolo[1,2,4]triazol-2-yl)-2H-chromen-2-one(ATTC) Molecule. Hittite Journal of Science and Engineering. 10, 11-19. https://doi.org/10.17350/HJSE19030000286
- Bağlan, M., Gören, K., Yıldıko, Ü., 2023b. HOMO– LUMO, NBO, NLO, MEP analysis and molecular docking using DFT calculations in DFPA molecule.

- International Journal of Chemistry and Technology. 7, 38-47. https://doi.org/10.32571/ijct.1135173
- Bağlan, M., Yıldıko, Ü., Gören, K., 2022. Computational Investigation of 5.5",7"-trihydroxy-3,7-dimethoxy-4'-4"'-O-biflavone from Flavonoids Using DFT Calculations and Molecular Docking. Adıyaman University Journal of Science. 12, 283-298. https://doi.org/10.37094/adyujsci.1121018
- Bağlan, M., Yıldıko, Ü., Gören, K., 2023. DFT Calculations and Molecular Docking Study in 6-(2"-Pyrrolidinone-5"-Yl)-(-) Epicatechin Molecule from Flavonoids. Eskişehir Teknik Üniversitesi Bilim ve Teknoloji Dergisi B-Teorik Bilimler. 11, 43-55. https://doi.org/10.20290/estubtdb.1126604
- Baig, M.M., GholamHosseini, H., Moqeem, A.A., Mirza, F., Lindén, M., 2019. Clinical decision support systems in hospital care using ubiquitous devices: Current issues and challenges. Health Informatics J. 25, 1091-1104. 10.1177/1460458217740722
- Bakal, R.L., Jawarkar, R.D., Manwar, J.V., Jaiswal, M.S., Ghosh, A., Gandhi, A., Zaki, M.E.A., Al-Hussain, S., Samad, A., Masand, V.H., Mukerjee, N., Nasir Abbas Bukhari, S., Sharma, P., Lewaa, I., 2022. Identification of potent aldose reductase inhibitors as antidiabetic (Anti-hyperglycemic) agents using QSAR based virtual Screening, molecular Docking, MD simulation and MMGBSA approaches. Saudi Pharm J. 30, 693-710. 10.1016/j.jsps.2022.04.003
- Burley, S.K., Berman, H.M., Bhikadiya, C., Bi, C., Chen, L., Di Costanzo, L., Christie, C., Dalenberg, K., Duarte, J.M., Dutta, S., 2019. RCSB Protein Data Bank: biological macromolecular structures enabling research and education in fundamental biology, biomedicine, biotechnology and energy. Nucleic acids research. 47, D464-D474. https://doi.org/10.1093/nar/gky1004
- Çimen, E., Gören, K., Tahiroğlu, V., Yıldıko, Ü., 2025. The Theoretical Calculations by DFT Method and Analysis ADME, Molecular Docking of 1-(1-(4-hydroxybutyl)-6-methyl-4-phenyl-2-thioxohexahydropyrimidin-5-yl)ethan-1-one (pyrimidine-thiones) Compound. Osmaniye Korkut Ata Üniversitesi Fen Bilimleri Enstitüsü Dergisi. 8, 1129-1145.
- Çimen, E., Tahiroğlu, V., 2024. 3-[1-(5-Amino-[1, 3, 4] tiadiazol-2-il)-2-(1H-imidazol-4-il)-etilimino]-2,3-dihidro-indol-2-on Molekülün Teoriksel İncelenmesi. Türk Doğa ve Fen Dergisi. 13, 6-13.
- Er, M., Ahmadov, F., Karakurt, T., Direkel, Ş., Tahtaci, H., 2019. A Novel Class Substituted Imidazo [2, 1-b][1,3,4] thiadiazole Derivatives: Synthesis, Characterization, In Vitro Biological Activity, and Potential Inhibitors Design Studies. ChemistrySelect. 4, 14281-14290.
- G.W.T. M.J. Frisch, H.B.S., G.E. Scuseria, M.A. Robb, J.R. Cheeseman, G. Scalmani, V. Barone, B. Mennucci, G.A. Petersson, H. Nakatsuji, M.

- Caricato, X. Li, H.P. Hratchian, A.F. Izmaylov, J. Bloino, G. Zheng, J.L. Sonnenberg, M. Hada, M. Ehara, K. Toyota, R. Fukuda, J. Hasegawa, M. Ishida, T. Nakajima, Y. Honda, O. Kitao, H. Nakai, T. Vreven, J.A. Montgomery Jr., J.E. Peralta, F. Ogliaro, M. Bearpark, J.J. Heyd, E. Brothers, K.N. Kudin, V.N. Staroverov, R. Kobayashi, J. Normand, K. Raghavachari, A. Rendell, J.C. Burant, S.S. Iyengar, J. Tomasi, M. Cossi, N. Rega, J.M. Millam, M. Klene, J.E. Knox, J.B. Cross, V. Bakken, C. Adamo, J. Jaramillo, R. Gomperts, R.E. Stratmann, O. Yazyev, A.J. Austin, R. Cammi, C. Pomelli, J.W. Ochterski, R.L. Martin, K. Morokuma, V.G. Zakrzewski, G.A. Voth, P. Salvador, J.J. Dannenberg, S. Dapprich, A.D. Daniels, Ö. Farkas, J.B. Foresman, J.V. Ortiz, J. Cioslowski, D.J. Fox. (2009). Gaussian 09. In (Version Revision A.02)
- Gifty, V.,Jothy, V.B., 2023. Experimental and theoretical vibrational spectral Investigations, structural conformations, DFT estimations and docking studies of antibacterial drug Nitrilotriaceticacid. Journal of Molecular Liquids. 386, 122380.
- Gökce, H., Alpaslan, Y.B., Zeyrek, C.T., Ağar, E., Güder, A., Özdemir, N., Alpaslan, G., 2019. Structural, spectroscopic, radical scavenging activity, molecular docking and DFT studies of a synthesized Schiff base compound. Journal of Molecular Structure. 1179, 205-215.
- Gören, K.,Bağlan, M., 2023. Inflammation and Anti-Inflammatory Drugs. New Frontiers In Health Sciences. 59.
- Gören, K., Bağlan, M., Tahiroğlu, V., Yıldıko, Ü., 2024. Theoretical Calculations and Molecular Docking Analysis of 4-(2-(4-bromophenyl)hydrazineylidene)-3,5-diphenyl-4H-pyrazole Molecule. Journal of Advanced Research in Natural and Applied Sciences. 10, 786-802. https://doi.org/10.28979/jarnas.1516154
- Gören, K., Bağlan, M., Yıldıko, Ü., 2024a. Antimicrobial, and Antitubercular Evaluation with ADME and Molecular Docking Studies and DFT Calculations of (Z)-3-((1-(5-amino-1,3,4-thiadiazol-2-yl)-2-Phenylethyl)imino)-5-nitroindolin-2-one Schiff Base. Karadeniz Fen Bilimleri Dergisi. 14, 1694-1708. https://doi.org/10.31466/kfbd.1423367
- Gören, K., Bağlan, M., Yıldıko, Ü., 2024b. Melanoma Cancer Evaluation with ADME and Molecular Docking Analysis, DFT Calculations of (E)-methyl 3-(1-(4-methoxybenzyl)-2,3-dioxoindolin-5-yl)-acrylate Molecule. Journal of the Institute of Science and Technology. 14, 1186-1199. https://doi.org/10.21597/jist.1467666
- Gören, K., Bağlan, M., Yıldıko, Ü., 2025. Analysis by DFT, ADME and Docking Studies of N'-(4-hydroxy-3-methoxybenzylidene)naphtho[2,3-b]furan-2-carbohydrazide. Eskişehir Teknik Üniversitesi Bilim ve Teknoloji Dergisi B-Teorik Bilimler.13,7-23.

- Gören, K., Kotan, G., Manap, S., Yüksek, H., 2024. Synthesis, Antimicrobial and Antioxidant Activities of 3-Alkyl(aryl)-4-(3-methoxy-4-hydroxybenzylideneamino)-4,5-dihydro-1*H*-1,2,4-triazol-5-one Derivatives. Chemistry Africa. 7, 5273-5289. https://doi.org/10.1007/s42250-024-01139-2
- Gören, K.,Yıldıko, Ü., 2024. Aldose Reductase Evaluation against Diabetic Complications Using ADME and Molecular Docking Studies and DFT Calculations of Spiroindoline Derivative Molecule. Süleyman Demirel Üniversitesi Fen Bilimleri Enstitüsü Dergisi. 28, 281-292. https://doi.org/10.19113/sdufenbed.1474689
- Güller, P., Taşer, B., Özkan, H., 2025. Exploring the Antibacterial and Enzyme Inhibitory Potential of Selected β-Carboline Derivatives: In Vitro and In Silico Insights. International Journal of Chemistry and Technology. 9, 13-24. 10.32571/ijct.1648820
- Hagar, M., Ahmed, H.A., Aljohani, G., Alhaddad, O.A., 2020. Investigation of some antiviral N-heterocycles as COVID 19 drug: molecular docking and DFT calculations. International Journal of Molecular Sciences. 21, 3922. https://doi.org/10.3390/ijms21113922
- Hajam, T.A., Saleem, H., Syed Ali Padhusha, M.,
 Mohammed Ameen, K., 2022. Quantum mechanical study, spectroscopic (FT-IR, FT-Raman and UV-Vis) study, NBO, NLO analysis and molecular docking studies of 2-ethoxy-4-(pyridine-2yliminomethyl)-phenol. Polycyclic Aromatic Compounds. 42, 4819-4842.
- Hassan, S.A., Aziz, D.M., Kader, D.A., Rasul, S.M., Muhamad, M.A., Muhammedamin, A.A., 2025. Design, synthesis, and computational analysis (molecular docking, DFT, MEP, RDG, ELF) of diazepine and oxazepine sulfonamides: biological evaluation for in vitro and in vivo anti-inflammatory, antimicrobial, and cytotoxicity predictions. Molecular Diversity. 29, 2367-2389. https://doi.org/10.1007/s11030-024-10996-5
- Kaya, B., Acar Çevik, U., Necip, A., Duran, H.E., Çiftçi, B., Işık, M., Soyer, P., Bostancı, H.E., Kaplancıklı, Z.A., Beydemir, Ş., 2025. Design, Synthesis, Biological Evaluation, and Molecular Docking Studies of Novel 1,3,4-thiadiazole derivatives targeting both aldose reductase and α-glucosidase for diabetes mellitus. ACS Omega. 10, 18812-18828. 10.1021/acsomega.5c00566
- Kredzielak-Manikowska, I., Traczyk, Z., Ceglarek, B., Sikorska, A., Brycz-Witkowska, J., Stańczak, H., Wozniak, J., Konopka, L., 2000. [Chronic eosinophilic leukemia]. Pol Arch Med Wewn. 103, 67-71.
- Kumar, B., Devi, J., Dubey, A., Tufail, N., Khurana, D., 2024. Thiosemicarbazone ligands based transition metal complexes: a multifaceted investigation of antituberculosis, anti-inflammatory, antibacterial, antifungal activities, and molecular docking, density

- functional theory, molecular electrostatic potential, absorption, distribution, metabolism, excretion, and toxicity studies. Applied Organometallic Chemistry. 38, e7345. https://doi.org/10.1002/aoc.7345
- Lee, Y.S., Chen, Z., Kador, P.F., 1998. Molecular modeling studies of the binding modes of aldose reductase inhibitors at the active site of human aldose reductase. Bioorg Med Chem. 6, 1811-1819. 10.1016/s0968-0896(98)00139-4
- Li, X., Keady, J., Ward, R., 2021. Neighbourhoods and dementia: An updated realist review of the qualitative literature to inform contemporary practice and policy understanding. Dementia (London). 20, 2957-2981. 10.1177/14713012211023649
- Lin, J., Sahakian, D.C., De Morais, S., Xu, J.J., Polzer, R.J., Winter, S.M., 2003. The role of absorption, distribution, metabolism, excretion and toxicity in drug discovery. Current topics in medicinal chemistry. 3, 1125-1154.
- Liu, N.Q., Cao, M., Frédérich, M., Choi, Y.H., Verpoorte, R., van der Kooy, F., 2010. Metabolomic investigation of the ethnopharmacological use of Artemisia afra with NMR spectroscopy and multivariate data analysis. J Ethnopharmacol. 128, 230-235. 10.1016/j.jep.2010.01.020
- Nishida, A., Kubota, T., Yamada, Y., Higashi, K., Kitamura, K., Nakahara, K., Iga, T., 2002. Thiopurine S-methyltransferase activity in Japanese subjects: metabolic activity of 6-mercaptopurine 6-methylation in different TPMT genotypes. Clin Chim Acta. 323, 147-150. 10.1016/s0009-8981(02)00184-5
- Noureddine, O., Issaoui, N., Al-Dossary, O., 2021. DFT and molecular docking study of chloroquine derivatives as antiviral to coronavirus COVID-19. Journal of King Saud University-Science. 33, 101248. https://doi.org/10.1016/j.jksus.2020.101248
- Patel, H.M., Noolvi, M.N., Sethi, N.S., Gadad, A.K., Cameotra, S.S., 2017. Synthesis and antitubercular evaluation of imidazo [2,1-b][1,3,4] thiadiazole derivatives. Arabian Journal of Chemistry. 10, S996-S1002. https://doi.org/10.1016/j.ejmech.2015.03.024
- Ramprasad, J., Nayak, N., Dalimba, U., Yogeeswari, P., Sriram, D., Peethambar, S., Achur, R., Kumar, H.S., 2015. Synthesis and biological evaluation of new imidazo [2,1-b][1,3,4] thiadiazole-benzimidazole derivatives. European journal of medicinal chemistry. 95, 49-63.
- Release, S., 2019. 3: Maestro, Schrödinger, LLC: New York, NY, USA. 2019.
- Romagnoli, R., Baraldi, P.G., Prencipe, F., Balzarini, J., Liekens, S., Estévez, F., 2015. Design, synthesis and antiproliferative activity of novel heterobivalent hybrids based on imidazo [2,1-b][1,3,4] thiadiazole and imidazo [2,1-b][1,3] thiazole scaffolds. European journal of medicinal chemistry. 101, 205-217.

- Sakthivel, S., Alagesan, T., Muthu, S., Abraham, C.S., 2018. Quantum mechanical, Geetha, E., spectroscopic study (FT-IR and FT-Raman), NBO HOMO-LUMO, analysis, first hyperpolarizability and docking studies of a nonsteroidal anti-inflammatory compound. Journal of 1156. Molecular Structure. 645-656. https://doi.org/10.1016/j.molstruc.2017.12.024
- Saravanan, R., Seshadri, S., Gunasekaran, S., Mendoza-Meroño, R., García-Granda, S., 2015.
 Conformational analysis, X-ray crystallographic, FT-IR, FT-Raman, DFT, MEP and molecular docking studies on 1-(1-(3-methoxyphenyl)ethylidene) thiosemicarbazide. Spectrochimica Acta Part A: Molecular and Biomolecular Spectroscopy. 139, 321-328.
- Satheeshkumar, R., Prabha, K., Vennila, K.N., Sayin, K., Güney, E., Kaminsky, W., Acevedo, R., 2022. Spectroscopic (FT-IR, NMR, single crystal XRD) and DFT studies including FMO, Mulliken charges, and Hirshfeld surface analysis, molecular docking and ADME analyses of 2-amino-4′-fluorobenzophenone (FAB). Journal of Molecular Structure. 1267, 133552. https://doi.org/10.1016/j.molstruc.2022.133552
- Shahabi, D., Tavakol, H., 2017. DFT, NBO and molecular docking studies of the adsorption of fluoxetine into and on the surface of simple and sulfur-doped carbon nanotubes. Applied Surface Science. 420, 267-275. https://doi.org/10.1016/j.apsusc.2017.05.068
- Shalaby, M.A., Fahim, A.M., Rizk, S.A., 2023. Microwave-assisted synthesis, antioxidant activity, docking simulation, and DFT analysis of different heterocyclic compounds. Scientific Reports. 13, 4999.
- Srivastava, V., Yadav, A., Sarkar, P., 2022. Molecular docking and ADMET study of bioactive compounds of Glycyrrhiza glabra against main protease of SARS-CoV2. Materials Today: Proceedings. 49, 2999-3007.
 - https://doi.org/10.1016/j.matpr.2020.10.055
- Systèmes, D., 2016. Biovia, discovery studio modeling environment. Dassault Systèmes Biovia: San Diego, CA, USA.
- Tahiroğlu, V., Gören, K., Bağlan, M., 2025. In Silico drug evaluation by molecular docking, ADME studies and DFT calculations of 2-(6-chloro-2-(4-chlorophenyl)imidazo[1,2-a]pyridin-3-yl)-N,N-dipropylacetamide. BMC Pharmacology and Toxicology. 26, 116. https://doi.org/10.1186/s40360-025-00958-4
- Tahiroğlu, V., Gören, K., Bağlan, M., Yıldıko, Ü., 2024.
 Molecular Docking and DFT Analysis of Thiazolidinone-Bis Schiff Base for anti-Cancer and anti-Urease Activity. Journal of the Institute of Science and Technology. 14, 822-834. https://doi.org/10.21597/jist.1416223

- Tahiroğlu, V., Gören, K., Çimen, E., Yıldıko, Ü., 2024. Moleculer Docking and Theoretical Analysis of the (E)-5-((Z)-4-methylbenzylidene)-2-(((E)-4-methylbenzylidene)hydrazineylidene)-3-phenylthiazolidin-4-one Molecule. Bitlis Eren Üniversitesi Fen Bilimleri Dergisi. 13, 659-672. https://doi.org/10.17798/bitlisfen.1471235
- Tahiroğlu, V., Gören, K., Kotan, G., Yüksek, H., 2025. In silico drug evaluation by molecular docking, ADME studies and synthesis, characterization, biological activities, DFT, SAR analysis of the novel Mannich bases. BMC Chemistry. 19, 249. https://doi.org/10.1186/s13065-025-01615-x
- Tahiroğlu, V., Gören, K., Yıldıko, Ü., Bağlan, M., 2024. IInvestigation, Structural Characterization and Evaluation of the Biological Potency by Molecular Docking of Amoxicillin Analogue of a Schiff Base Molecule. International Journal of Chemistry and Technology.

 8, 190-199. https://doi.org/10.32571/ijct.1410570
- Umamaheswari, M., Aji, C., Asokkumar, K., Sivsshanmugam, T., Subhadradevi, V., Jagannath, P., Madeswaran, A., 2012. Docking studies: In silico aldose reductase inhibitory activity of commercially available flavonoids. Bangladesh Journal of Pharmacology. 7, 108-113.
- Uzzaman, M., Hasan, M.K., Mahmud, S., Yousuf, A., Islam, S., Uddin, M.N., Barua, A., 2021. Physicochemical, spectral, molecular docking and ADMET studies of Bisphenol analogues; A computational approach. Informatics in medicine unlocked. 25, 100706. https://doi.org/10.1016/j.imu.2021.100706
- Yadav, D.K., Kumar, S., Saloni, Singh, H., Kim, M.-h., Sharma, P., Misra, S., Khan, F., 2017. Molecular docking, QSAR and ADMET studies of withanolide analogs against breast cancer. Drug Design, Development and Therapy. 1859-1870. https://doi.org/10.2147/DDDT.S130601
- Zaki, Y.H., Abdelhamid, A.O., Sayed, A.R., Mohamed, H.S., 2023. Synthesis of 1, 3, 4-thiadiazole derivatives using hydrazonoyl bromide: Molecular docking and computational studies. Polycyclic Aromatic Compounds. 43, 1364-1377.